

1 ***Quantum pBac: An effective, high-capacity piggyBac-based gene***
2 ***integration vector system for unlocking gene therapy potential***

3 Wei-Kai Hua^{1,*}, Jeff C. Hsu^{1,*}, Yi-Chun Chen^{1,*}, Peter S. Chang¹, Kuo-Lan Karen
4 Wen¹, Po-Nan Wang², Yi-Shan Yu¹, Ying-Chun Chen¹, I-Cheng Cheng¹, Sareina
5 Chiung-Yuan Wu^{1,†}

6 ¹GenomeFrontier Therapeutics, Inc. Taipei City, Taiwan (R.O.C.)

7 ²Division of Hematology, Chang Gung Medical Foundation, Linkou Branch,
8 Taipei City, Taiwan (R.O.C.)

9 * These authors contributed equally to this work and their authorship order is
10 interchangeable

11

12 †Correspondence should be addressed to:

13 S.C.-Y.W. (sareina@genomefrontier.com) 18F-1, No. 3, Park St., Nangang Dist.,
14 Taipei City 11503, Taiwan (R.O.C.); +886-2-26558766;

15 This work was performed in Taipei City, Taiwan (R.O.C.)

16 Short title: *Quantum pBac* for unlocking gene therapy potential

17 **Abstract**

18 Recent advances in gene therapy have brought novel treatment options to
19 cancer. However, safety concerns and limited payload capacity in commonly-
20 utilized viral vectors prevent researchers from unlocking the full potential of gene
21 therapy. Virus-free DNA transposons, including *piggyBac*, have been shown to
22 obviate these shortcomings. We have previously demonstrated superior
23 transposition efficiency of a modified *piggyBac* system. Here, we further advanced
24 this modified *piggyBac* system and demonstrated that the internal domain
25 sequences (IDS) within 3' terminal repeat domain of hyperactive *piggyBac* (*hyPB*)
26 donor vector contain dominant enhancer elements. We showed that a plasmid-
27 free donor vector devoid of IDS in conjunction with a helper plasmid expressing
28 *Quantum pBase*[™] v2 form the most optimal *piggyBac* system, *Quantum pBac*[™]
29 (*qPB*), in T cells. We further demonstrated that cells transfected with *qPB*
30 expressing CD20/CD19 CAR outperformed cells transfected with the same donor
31 vector but with plasmid expressing *hyPB* transposase in CAR-T cell production.
32 Importantly, we showed that *qPB* produced mainly CD8⁺ CAR-T_{SCM} cells. These
33 CAR-T cells effectively eliminated CD20/CD19-expressing tumor cells *in vitro* and
34 *in vivo*. Our findings confirm *qPB* as a promising virus-free vector system that is

35 safer, and highly efficient in mediating transgene integration with the payload

36 capacity to incorporate multiple genes.

37

38 Keywords: gene therapy | transposon | *piggyBac* | CAR-T

39

40 **Introduction**

41 It has been well documented that almost all human diseases occur due to
42 genetic defects. Gene therapy is the administration of genetic materials (i.e. DNA
43 or RNA) to alter the biological properties of living cells for treating diseases¹. Thus,
44 theoretically, gene therapy has the potential to cure most, if not all, diseases via a
45 single treatment. Building upon decades of scientific, clinical, and manufacturing
46 advances, gene therapy is now bringing novel treatment options to multiple fields
47 of medicine, including cancer and genetic disorders.

48 Gene therapy often requires stable, long-term expression of therapeutic
49 transgene(s) in cells. This is accomplished by engineering cells using viral or non-
50 viral vector systems, either *ex vivo* or *in vivo*. Viral vectors are most commonly
51 used for gene therapy due to their high efficiencies in gene delivery and integration,
52 resulting in stable and long-term gene expression. However, viral vectors have
53 several intrinsic limitations. These include (1) limited payload capacity that
54 severely restricts the repertoire of genes that can be integrated²; (2) genotoxicity
55 arising from preferential integration into sites near or within active gene loci that
56 may negatively impact the expression and/or function(s) of genes³⁻⁸; (3) the
57 proclivity of silencing genes introduced by viral vectors, presumably due to cellular
58 immunity^{9,10}; and (4) safety concerns related to immunogenicity of viral vectors¹¹.
59 Additionally, production of viral vectors for clinical trials is costly, time consuming
60 (> 6 months), and supply-constrained, which in turn represent a significant hurdle
61 in routine medical practice¹².

62 In recent years, in conjunction with the technology advancement of non-
63 viral gene delivery, virus-free DNA transposons have been shown to be capable
64 of obviating these shortcomings and emerged as a promising vector system for
65 gene therapy^{13,14}, due to its effective gene integration capability¹⁵. DNA
66 transposons, also known as mobile elements or jumping genes, are genetic
67 elements with the ability to transverse in the genome via a “cut-and-paste”
68 mechanism. In nature, a simple DNA transposon contains a transposase gene
69 flanked by terminal repeat sequences. During the transposition process, the ability
70 of transposase to act *in trans* on virtually any DNA sequence that is flanked by the
71 terminal repeat sequences makes DNA transposons particularly attractive as gene
72 delivery tools for gene therapy. To turn DNA transposon into a tool for genetic
73 engineering, a controllable bi-component vector system consisting of (1) a helper
74 plasmid expressing the transposase and (2) a donor plasmid with exogenous DNA
75 of interest flanked by the transposon terminal repeat sequences, was developed.
76 Currently, *Sleeping Beauty* and *piggyBac* have been identified as the most
77 promising DNA transposons for human gene therapy and have been clinically
78 explored as vectors for several CAR-T cell therapies. Unlike *Sleeping Beauty*
79 which was reconstructed from salmon genome^{16,17}, *piggyBac* derived from the
80 cabbage looper moth *Trichoplusia ni* is naturally active in humans^{18–20}. By
81 introducing amino acid mutations to the transposase, a *hyPB* transposase,
82 *hyPB*ase, and two hyperactive transposases of *Sleeping Beauty*, SB100X and
83 hyperactive SB100X (30% more active than SB100X) were developed^{21–25}. When
84 exogenous gene is *ex vivo* delivered to primary human T cells, *hyPB*ase increased

85 gene delivery rate by two to three folds, compared with *piggyBac* and SB100X
86 transposases. Previously, by shortening of the *piggyBac* terminal repeat domain
87 (TRD) sequences, we have observed a 2.6-fold increase in transposition activity
88 mediated by *piggyBac* in HEK293 cells²⁶. We have also demonstrated that
89 *hyPBase* activity can be further improved by two to three folds after fusing
90 *hyPBase* with various peptides²⁷. In this study, we address whether the *piggyBac*
91 system can be further developed for therapeutic application. We demonstrate that
92 *qPB*, a binary *piggyBac* system comprising a plasmid-free donor vector and a
93 helper plasmid expressing *Quantum pBase*[™] (*qPBase*) v2, a molecularly-
94 engineered *hyPBase*, is a simple yet robust and potentially safest vector system
95 for generating potent CD19/CD20 dual-targeting CAR-T cells for treatment of B
96 cell malignancies.

97

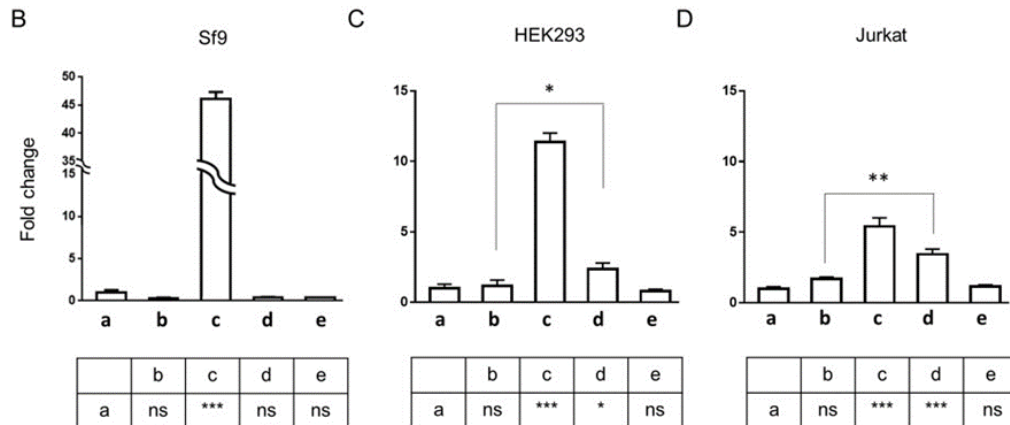
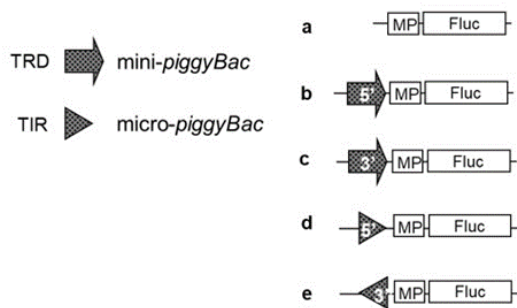
98 **Results**

99 **Micro-*piggyBac* possesses significantly lower enhancer activity compared** 100 **to mini-*piggyBac***

101 Malignancies caused by vector-mediated insertional activation of proto-
102 oncogenes was evident in the initial clinical trial of retrovirus-based gene therapy
103 for SCID-X1. The currently available minimal *piggyBac* transposon vector,
104 designated as mini-*piggyBac* here, is composed of *cis* elements 5' (244 bp) and 3'
105 (313 bp) TRD, which are transposed along with gene of interest into the genome.
106 Each TRD contains a TIR sequence and an internal domain sequence (IDS). To
107 minimize the potential risk of insertional mutagenesis caused by gene delivery

108 vectors in gene therapy, we had previously generated *micro-piggyBac*, which
 109 contains the 5' (40 bp) and 3' (67 bp) TIR sequences of *mini-piggyBac*, while the
 110 respective IDS were removed²⁶. However, it remains unclear whether the TRDs
 111 of *mini-piggyBac* and/or TIRs of *micro-piggyBac* harbor enhancer and/or silencer
 112 activity. To address this issue, luciferase activities of a panel of reporter constructs
 113 containing individual TRD or TIR sequence was generated and examined in insect
 114 Sf9 cells, human HEK293 cells, and human Jurkat T cells (Figure 1).

A



128

129 **Figure 1. Enhancer/silencer activity of mini-*piggyBac* TRDs and micro-*piggyBac* TIRs**

130 (A) A schematic depiction showing a panel of luciferase reporter constructs containing a CMV
131 minimal promoter (MP) and firefly luciferase (*Fluc*) gene, with or without the 5' or 3' TRDs from
132 mini-*piggyBac* or 5' or 3' TIRs from micro-*piggyBac* inserted upstream of MP. Luciferase activities
133 exhibited by the reporter constructs of (A) in (B) Sf9, (C) HEK293, and (D) Jurkat cells. Results are
134 shown as mean fold changes in luciferase activity \pm standard deviation (SD; normalized first to
135 Renilla luciferase activity and then to the luciferase activity obtained from cells transfected with
136 construct a). Statistical analysis results of differences in fold change between luciferase activity
137 obtained from cells transfected with construct a and those from cells transfected with constructs b-
138 e are summarized in the lower panels (boxed regions). * $p < 0.05$, ** $p < 0.01$, *** $p < 0.001$. N = 3
139 (triplicates).

140

141 Compared to the control (Figure 1A, construct a), the 3' TRD of mini-
142 *piggyBac* (construct c) but not 3' TIR of micro-*piggyBac* (construct e) produced
143 significantly higher luciferase activity across all three cell types (Figure 1B-1D),
144 suggesting that enhancer activity is present in the 3' IDS of mini-*piggyBac*. On the
145 other hand, a slight yet significantly-enhanced luciferase activity was detected in
146 5' TIR of micro-*piggyBac* but not 5' TRD of mini-*piggyBac* in both HEK293 and
147 Jurkat cells. This suggests the presence of a minimal level of enhanced activity in
148 the 5' TIR and/or silencer activity in the 5' IDS of TRD (Figure 1B-1D). Taken
149 together, micro-*piggyBac* possesses significantly lower enhancer activity
150 compared to mini-*piggyBac*.

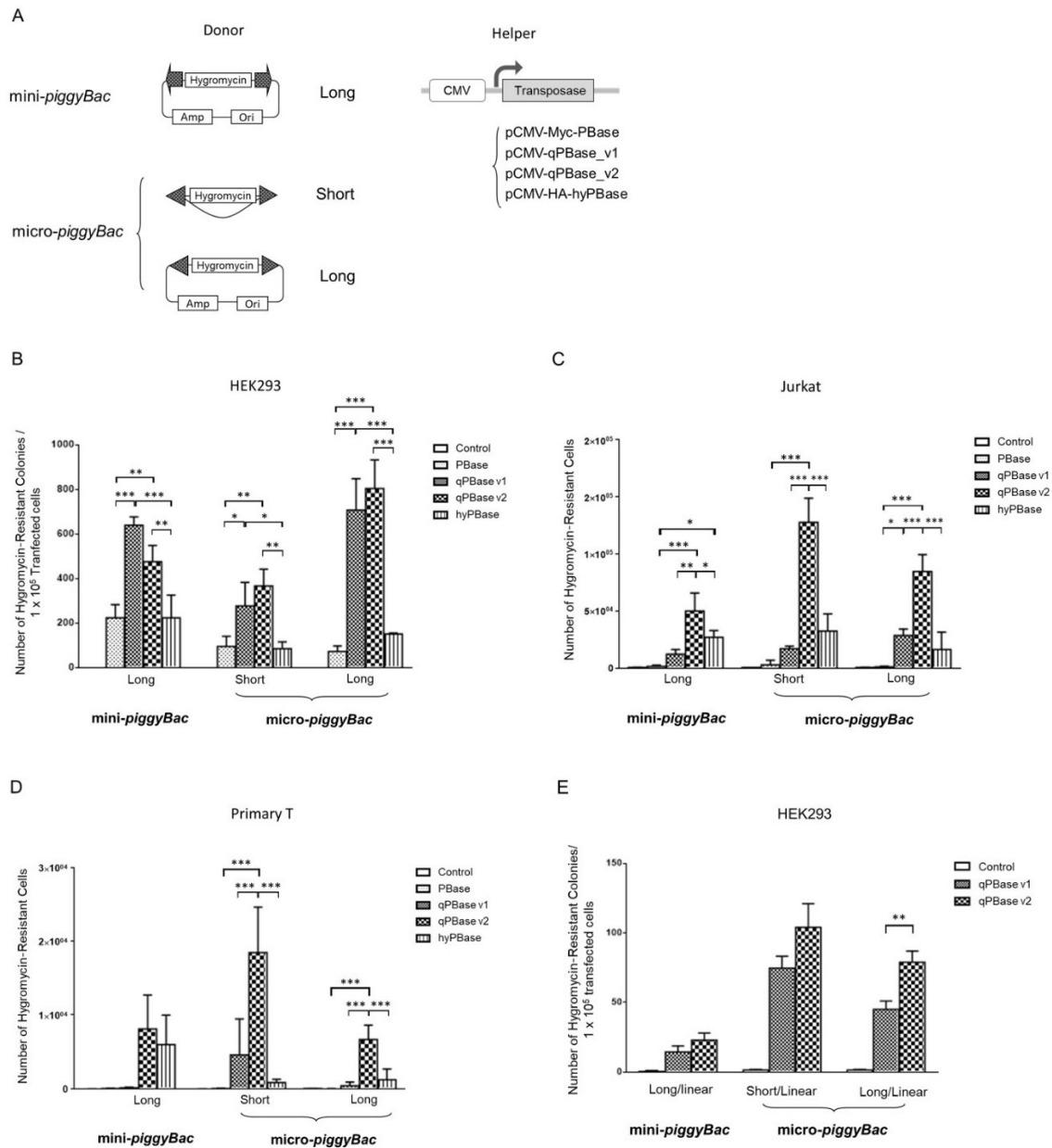
151

152 **Shortening of donor vector backbone in combination with *Quantum pBase*[™]**
153 **(*qPBase*) v2 enhances the transposition activity of micro-*piggyBac* in T cells**

154 The significantly-reduced enhancer activity of TIRs suggests that micro-
155 *piggyBac* is much safer for gene therapy applications. We therefore focused on
156 micro-*piggyBac* and determined whether its transposition activity may be further
157 enhanced by shortening the donor vector backbone, that is sequences outside of
158 the TIR-spanning region. We constructed two donor vectors named micro-
159 *piggyBac*-Short and micro-*piggyBac*-Long. Both of these vectors contain TIRs
160 (micro) and either retains in its backbone the replication components, namely
161 replication origin and antibiotic genes (Long), or is devoid of them (Short). A third
162 donor vector, mini-*piggyBac* Long, which contains TRDs (mini) and retains the
163 replication components in its backbone (Long), was also constructed for
164 comparison since its combination with helper plasmid expressing *hyPBase*
165 (commonly collectively referred to as “hyperactive *piggyBac*” or “*hyPB*”) is currently
166 the most advanced *piggyBac* system available (Figure 2A). We determined and
167 compared the transposition efficiency of these donor vectors used in combination
168 with helper plasmids expressing wild type *PBase* (pCMV-Myc-*PBase*), *hyPBase*
169 (pCMV-HA-*hyPBase*), and *qPBase* v1 or v2 (pCMV-*qPBase_v1* and pCMV-
170 *qPBase_v2*, respectively; Figure 2A).

171 As shown, *hyPBase*, either in combination with mini-*piggyBac*-Long or
172 micro-*piggyBac*-Short or -Long, mediated markedly-enhanced transposition
173 compared to *PBase* in T cells but not in HEK293 cells. *qPBase* v1, on the other

174 hand, mediated markedly-enhanced transposition compared to *hyPBase* in



175

176

177 **Figure 2. Transposition activity of various donor vector and helper plasmid combinations in**
 178 **human cells**

179 (A) A schematic depiction showing the *piggyBac* system with various donor vectors and helper
 180 plasmids as indicated. Transposition activity of the indicated combination of donor vector and
 181 helper plasmid in (B) HEK293, (C) Jurkat, and (D) primary T cells. (E) Transposition activity of the

182 indicated combination of linearized donor vector and helper plasmid in HEK293 cells. Results are
183 shown as mean number of hygromycin-resistant colonies/ 1×10^5 transfected cells \pm SD (B and E),
184 and mean number of hygromycin-resistant cells \pm SD (C and D). * $p < 0.05$, ** $p < 0.01$, *** $p <$
185 0.001. N = 3 (triplicates).

186

187 HEK293, but not so much in T cells (Figure 2B-2D). These results suggest that the
188 transposition activity of *hyPB*ase and *qPB*ase v1 are likely cell type-dependent.
189 We also found that *qPB*ase v2 mediated the highest transposition activity in almost
190 all of the tested combinations and cell types. Importantly, when *qPB*ase v2 is
191 accompanied by micro-*piggyBac*-Short donor vector, its transposition activity is by
192 far the highest in both Jurkat and primary T cells and is clearly superior to *hyPB*ase
193 in combination with mini-*piggyBac*-Long, that is *hyPB piggyBac* system (Figures
194 2C and 2D, respectively).

195 **Micro-*piggyBac* is superior to mini-*piggyBac* for advancing adeno-*piggyBac***
196 **hybrid vector for gene therapy**

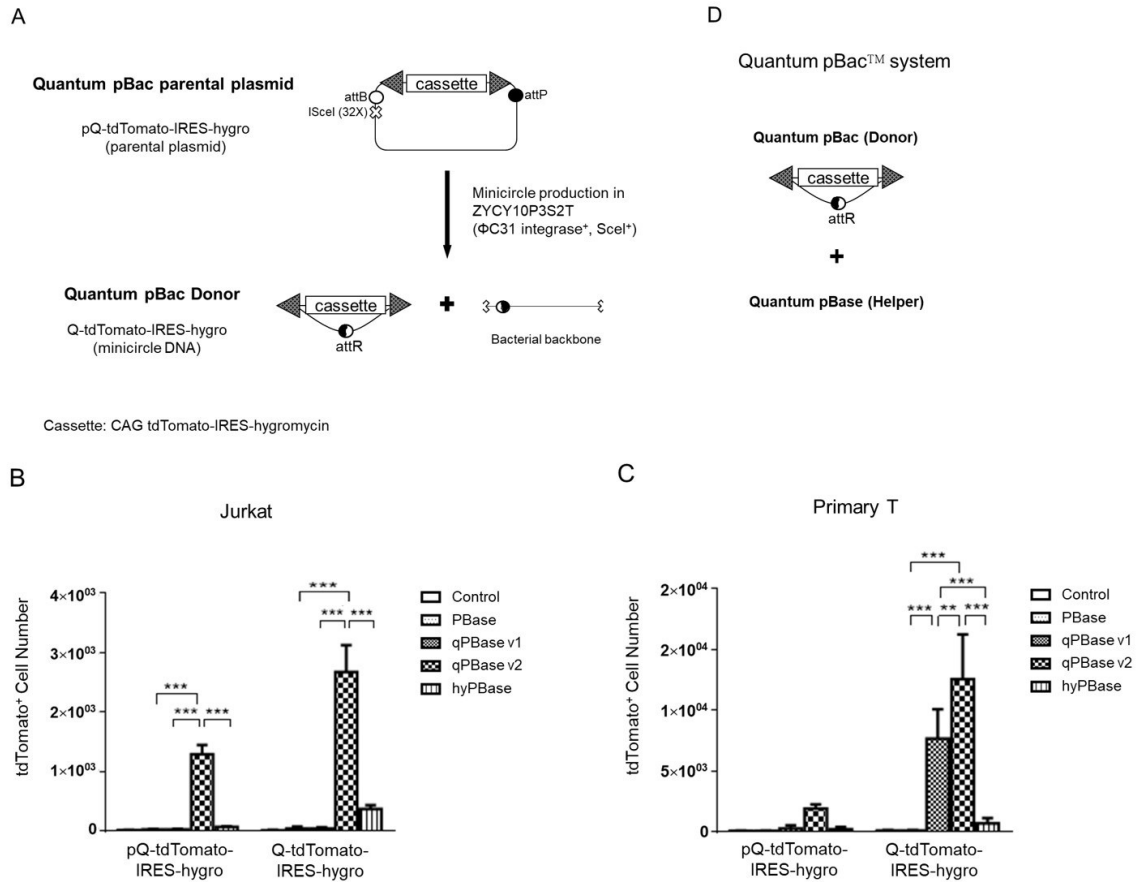
197 Even though *piggyBac* is capable of integrating sizable DNA (> 100 Kb), its
198 genome engineering efficiency is largely restricted by the effectiveness of gene
199 delivery methods. Electroporation is an effective virus-free gene delivery method
200 commonly used in gene therapy, but transfection efficiency is inversely correlated
201 with the size of DNA delivered due to elevating cell damages caused by
202 introduction of larger transgenes. Thus, to alleviate electroporation-associated
203 restriction imposed on the *piggyBac* system, an adenovirus-*piggyBac* hybrid
204 system, Ad-iPB7 was developed²⁸. Since the adenovirus genome exists in a linear

205 form, here we also examined the transposition activity of linearized forms of mini-
206 *piggyBac*-Long, micro-*piggyBac*-Short and micro-*piggyBac*-Long along with either
207 *qPBase v1* or *qPBase v2* to gain insights for future development of adenovirus-
208 *piggyBac* hybrid vector in gene therapy. As shown in Figure 2E, both micro-
209 *piggyBac*-Short and micro-*piggyBac*-Long are superior compared to mini-
210 *piggyBac*-Long. Moreover, when linearized micro-*piggyBac*-Long donor vector
211 was combined with *qPBase v2*, a significantly greater transposition efficiency was
212 observed compared to that produced when *qPBase v1* transposase was used
213 (Figure 2E).

214 **Minicircle micro-*piggyBac* is significantly more active than its parental**
215 **counterpart in both Jurkat and primary T cells**

216 Minicircle forms of DNA constructs offer several advantages, including
217 enhancements in gene delivery efficiency and stable transgene expression. These
218 advantages are due to the markedly reduced vector size of minicircle DNA as well
219 as the lack of both antibiotic resistant genes and gene silencing induced by
220 bacterial backbone sequences required for plasmid replication. We demonstrated
221 that removal of these backbone sequences outside of the TIR-spanning regions
222 via a cloning procedure (which shortens the size of the vectors) enhanced
223 transposition efficiency (Figure 2). Therefore, we next used the Mark Kay minicircle

224 system to generate a minicircle form of the donor vector (Q-tdTomato-IRES-hygro)
 225 from its parental plasmid counterpart (pQ-tdTomato-IRES-hygro) (Figure 3A)²⁹.



226
 227 **Figure 3. Transposition activity of various transposases with donor vector in parental**
 228 **plasmid or minicircle counterpart forms**

229 (A) A schematic depiction illustrating the generation of the *Quantum pBac*[™] (*qPB*) donor vector
 230 having a gene cassette carrying *tdTomato* and *hygro* genes linked by IRES (Q-tdTomato-
 231 IRES-hygro) from its parental plasmid (pQ-tdTomato-IRES-hygro). Transposition activity of the
 232 indicated combination of pQ-tdTomato-IRES-hygro or Q-tdTomato-IRES-hygro donor vector and
 233 helper plasmid in (B) Jurkat and (C) primary T cells. (D) A schematic depiction showing the two-
 234 component *qPB* system. Results are shown as mean number of tdTomato⁺ cells ± SD. ** p < 0.01,
 235 *** p < 0.001. N = 3 (triplicates).

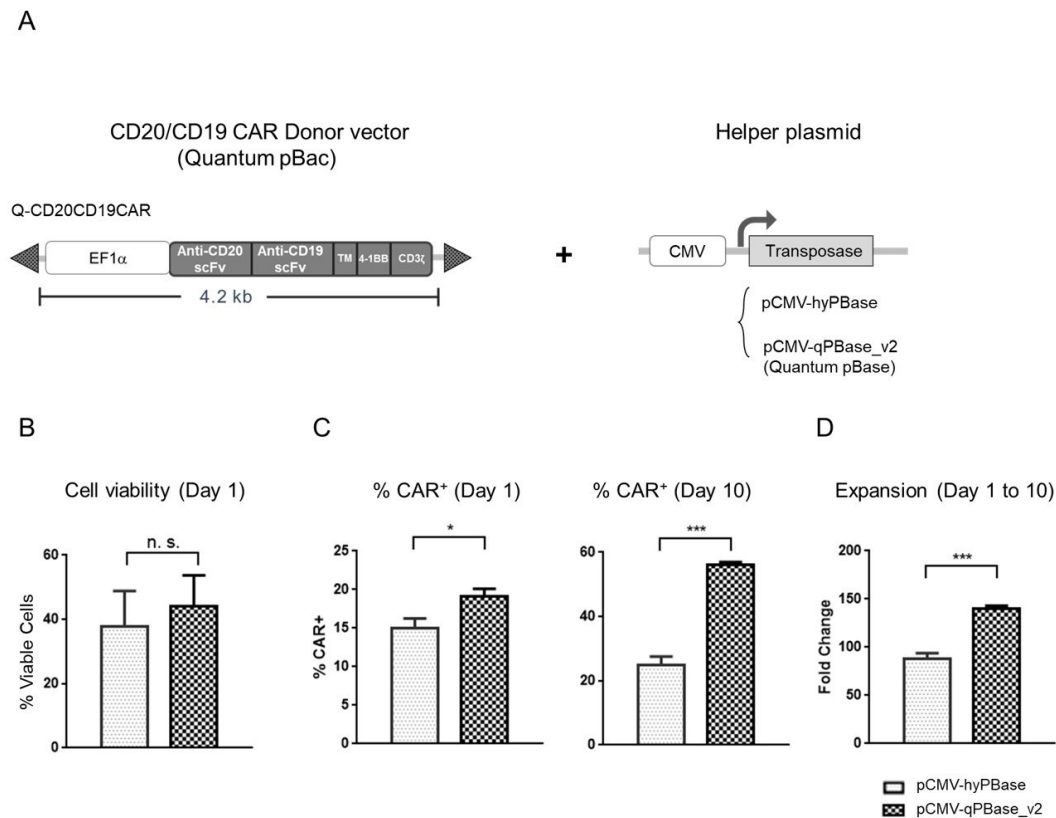
236 We determined whether donor vector produced using minicircle technology will
237 result in enhanced transposition efficiency similar to that produced by donor
238 vectors with backbone replication components removed by molecular cloning.

239 When donor vectors of parental plasmid (pQ-tdTomato-IRES-hygro) and
240 minicircle (Q-tdTomato-IRES-hygro) forms were compared, it was clear that
241 minicircle donor vector mediated markedly higher transposition efficiency than its
242 parental plasmid form, irrespective of the helper plasmid being co-electroporated.
243 Moreover, only cells co-electroporated with minicircle donor vector and helper
244 plasmid expressing *qPBase v2* consistently exhibited significantly higher
245 transposition activity compared to all other combinations, including those with the
246 helper plasmid expressing *hyPBase*. Based on these data in both Jurkat (Figure
247 3B) and primary T cells (Figure 3C), we selected micro-*piggyBac* vector in
248 minicircle DNA form as the donor vector and a series of recombinant *qPBase*

249 (*qPB* *v1* and *v2*) as the helper plasmid to form the *Qunatum pBac*TM (*qPB*)
250 system (Figure 3D).

251 **When combined with CD20/CD19 CAR *Qunatum pBac*TM (*qPB*) donor vector,**
252 ***Quantum pBase*TM (*qPB*) *v2* outperforms *hyPB*Base in CAR-T production**

253 We next evaluated the performance of *qPB* system using anti-CD20/CD19
254 CAR as the transgene cassette of *qPB* donor vector with helper plasmid that
255 encodes either *hyPB*Base or *qPB* *v2*. (Figure 4A).



256

257 **Figure 4. CAR-T cell production using *Qunatum pBac*TM (*qPB*) donor vector and helper**
258 **plasmid**

259 (A) A schematic depiction showing the CD20/CD19 CAR *qPB* donor vector and helper plasmid
260 pCMV-*hyPB*Base or pCMV-*qPB* *v2*. Characterization of (B) cell viability one day following
261 electroporation, (C) percentages of CAR⁺ cells on days 1 and 10 following electroporation, and (D)

262 fold expansion of cells after 10 days of culture. Results are shown as mean percentage of viable
263 cells \pm SD (B), mean percentage of CAR⁺ cells \pm SD (C), and mean fold change \pm SD (D). n.s. not
264 statistically significant, * $p < 0.05$, *** $p < 0.001$. N = 3 (triplicates).

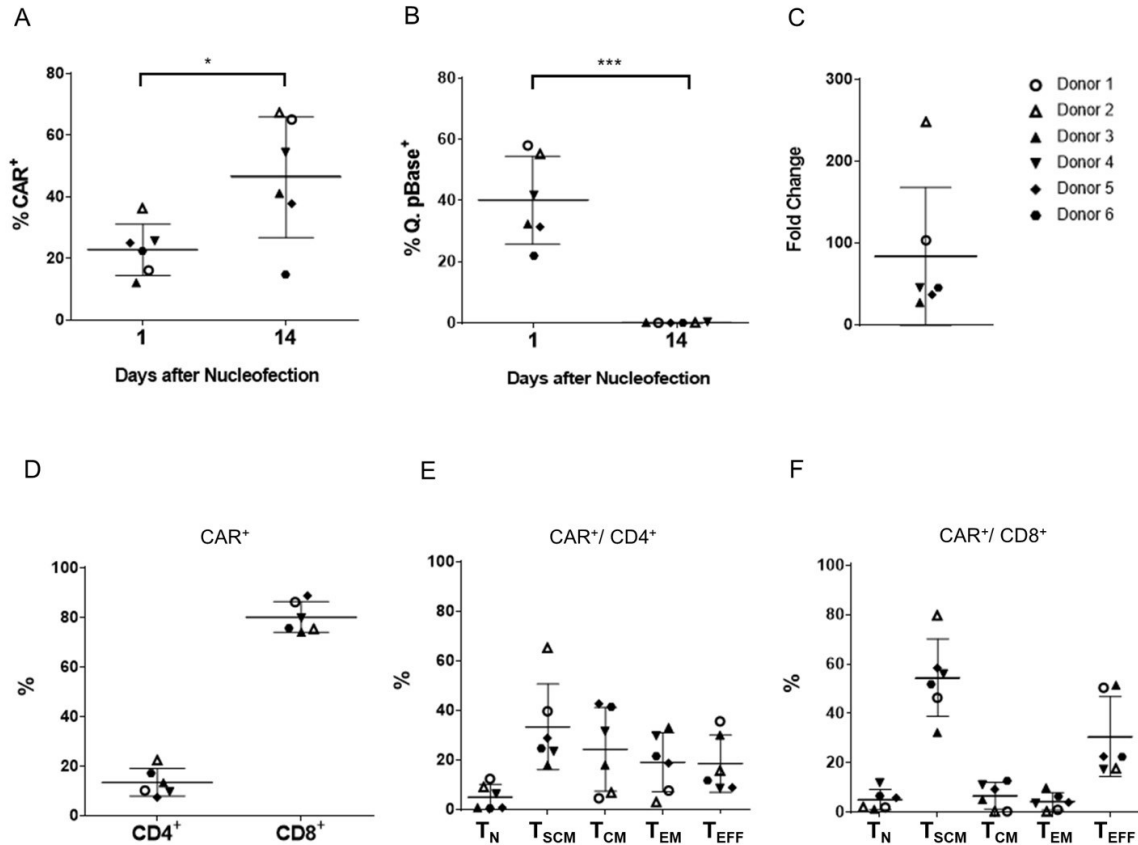
265

266 The viability of cells electroporated with CD20/CD19 CAR *qPB* donor vector and
267 helper plasmid expressing either *hyPB* or *qPB* v2 were not significantly
268 different one day after electroporation (Figure 4B). On the other hand, cells
269 electroporated with helper plasmid expressing *qPB* v2 resulted in significantly
270 more CAR⁺ cells than those electroporated with helper plasmid expressing
271 *hyPB* on day 1 after nucleofection (Figure 4C, left panel). This difference was
272 further amplified after 10 days of culture (Figure 4C, right panel), suggesting that
273 the transposition efficiency of *qPB* v2 is much higher than that of *hyPB*.
274 Moreover, the expansion of cells electroporated with CD20/CD19 CAR *qPB* donor
275 vector and helper plasmid expressing *qPB* v2 was also significantly higher than
276 that of cells electroporated with the same donor vector but with helper plasmid
277 expressing *hyPB* (Figure 4D). These observations suggest that the
278 transposition efficiency of *qPB* v2 is much higher than that of *hyPB*.

279 ***Qunatum pBac*[™] (*qPB*) system produces CAR⁺ T cells that are mainly of the**
280 **CD8⁺ subtype and are highly represented by the T_{scm} subset**

281 Next, we analyzed T cells derived from six healthy donors to determine
282 whether there may be donor-dependent variations in CAR⁺ cell production using
283 the *qPB* system (*qPB* donor vector with *qPB* v2 helper plasmid). The average
284 percentage of CAR⁺ T cells significantly increased from day 1 to 14 following

285 electroporation (Figure 5A), with only one of six donors (donor 6) exhibiting a
 286 decrease in percentage of CAR⁺ T cells.



287

288 **Figure 5. Characterization of healthy donor CAR-T cells produced using the *Qunatum***
 289 ***pBac*[™] (*qPB*) system**

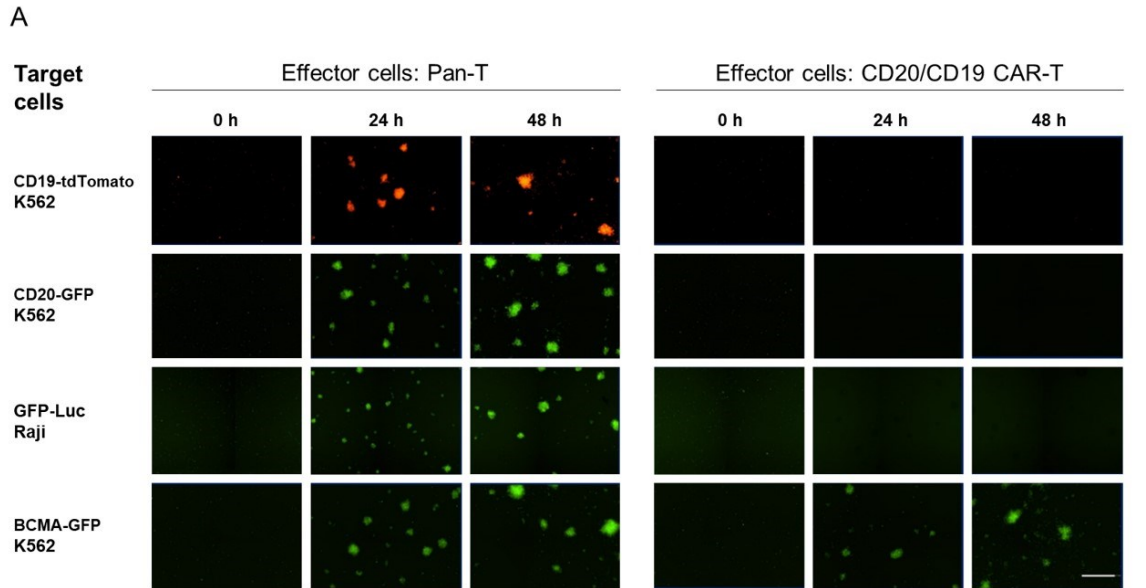
290 Percentages of (A) CAR⁺ and (B) transposase⁺ (*qPB*ase⁺) cells on days one and 14 following
 291 electroporation. (C) Fold expansion of cells after 14 days of culture. (D) Distribution of CD4⁺ and
 292 CD8⁺ T cell subtypes in CAR⁺ T cells. Distribution of five T cell differentiation subsets T_N, T_{SCM}, T_{CM},
 293 T_{EM} and T_{EFF} in (E) CD4⁺ CAR⁺ and (F) CD8⁺ CAR⁺ T cells on day 14. Results shown are from six
 294 healthy donors. Horizontal lines in (A, B, and D-F) represent the mean percentage of cells ± SD
 295 that are positive for the respective markers, and in (C) the mean fold change ± SD. * p < 0.05, ***
 296 p < 0.001. N = 6 PMBC donors.

297 Fourteen days after electroporation, the percentage of *qPBase*⁺ cells decreased
298 to minimal levels (< 0.4 %) in all of the donors (Figure 5B), suggesting successful
299 clearance of unwanted helper plasmids from T cells following completion of “cut-
300 and-paste” gene-integration function. There was high variability among the PBMC
301 donors (27-248 fold) in terms of the extent of CAR⁺ T cell expansion during the 14-
302 day culture period (Figure 5C), indicating a donor-dependent effect associated with
303 the expansion capacity of these cells. We also profiled the T cell subtypes (CD4⁺
304 and CD8⁺; Figure 5D) as well as T cell subsets based on differentiation stages
305 (Figure 5E, 5F) of CAR⁺ T cells derived from the PBMC donors. CD8⁺ T cells were
306 the major T cell subtype population (Figure 5D). Furthermore, T_{SCM} was the major
307 CAR⁺ T cell subset in both CD4 and CD8 populations (Figure 5E, 5F).

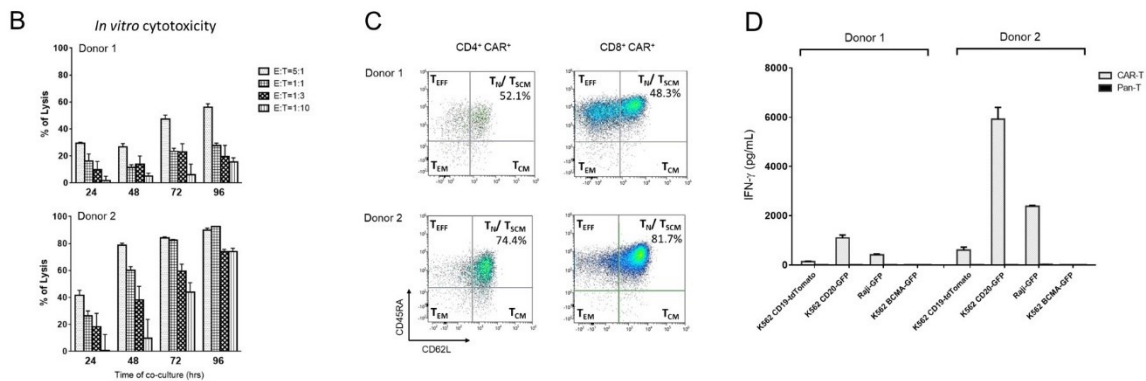
308 ***Qunatum pBac*TM (*qPB*) system produces functional CAR⁺ T cells that kill**
309 **target cells *in vitro***

310 We next determined whether CAR-T cells generated using the *qPB* system
311 (*qPB* donor vector with *qPBase* v2 helper plasmid) are functional in an *in vitro*
312 setting. As shown in Figure 6A, compared to pan-T cells, CD20/CD19 dual-
313 targeting CAR-T cells eradicated more CD19⁺CD20⁺ Raji cells (third row) and
314 K562 target cells engineered to express either CD19 (first row), or CD20 (second
315 row). On the other hand, CD20/CD19 dual-targeting CAR-T cells failed to eradicate
316 BCMA (irrelevant antigen)-expressing control K562 cells (fourth row). These
317 results demonstrated that the CAR-T cells specifically target and kill both CD20-
318 and CD19-expressing cells. The cytotoxic functions of CAR-T cells from two
319 donors (donor 1 and 2) were further assessed at different E:T ratios against Raji

320 cells. We observed dose- and time-dependent killing by CAR-T cells derived from
 321 both donors (Figure 6B).



322



323

324 **Figure 6. *In vitro* functional characterization of CAR-T cells produced using the *Quantum***
 325 ***pBac*[™] (*qPB*) system**

326 *In vitro* cytotoxicity results of Pan-T and/or CAR-T cells derived from healthy donor(s) (A) against
 327 the indicated target cells, and (B) at the indicated Effector: Target (E: T) ratio against Raji cells. (C)
 328 Representative flow cytometry data showing the distribution of T cell differentiation subsets
 329 T_N/T_{SCM}, T_{CM}, T_{EM} and T_{EFF} in CD4⁺ and CD8⁺ subtypes of donor 1 and donor 2 CAR⁺ T cells. (D)
 330 IFN- γ secretion by donor 1 and donor 2 CAR-T cells following antigen stimulation. Pan-T cells (non-

331 gene modified cells) served as a control group. Data shown in (B and D) represent the mean
332 percentage of cell lysis \pm SD and the mean IFN- γ concentration \pm SD, respectively. N = 3
333 (triplicates). Bar in (A) represents 500 μ m.

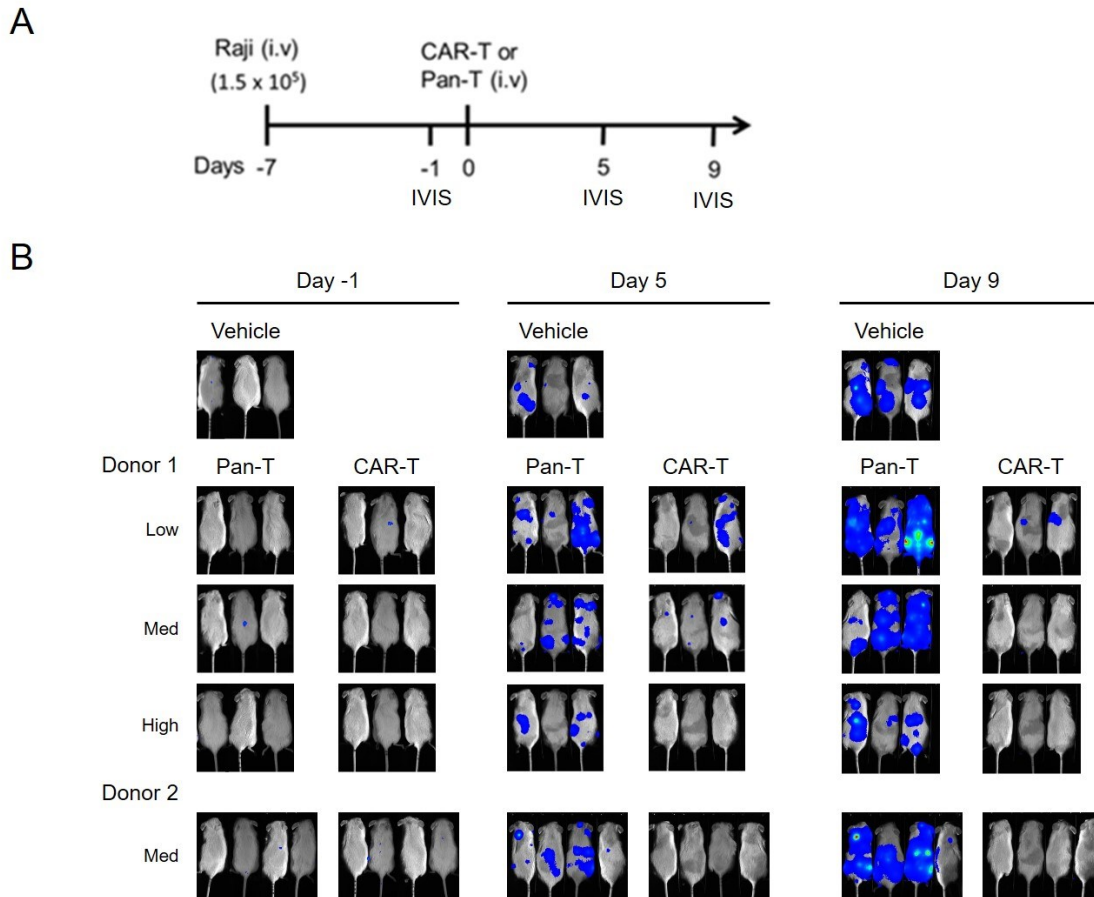
334

335 Donor 2 CAR-T cells were markedly more potent in killing Raji cells, which is
336 consistent with the higher level of IFN- γ detected in the 48-hour culture medium of
337 donor 2 CAR-T cells compared with that of donor 1 CAR-T cells (Figure 6D).
338 Notably, 74% of Raji cells were killed by donor 2 CAR-T cells after a 96-hour co-
339 culture period even at a E:T ratio of 1:10 (Figure 6B). This is in contrast to the
340 15.5% killing of Raji cells by donor 1 CAR-T cells at the same E:T ratio, these
341 results suggest a higher level of persistence in CAR-T cells derived from donor 2
342 as compared with those from donor 1. Supporting this notion, the percentages of
343 CAR⁺ T_{SCM} were higher in donor 2 (74.4% and 81.7% for CD4⁺ and CD8⁺ cells,
344 respectively) compared to donor 1 (52.1% and 48.3% for CD4⁺ and CD8⁺ cells,
345 respectively; Figure 6C).

346 **Effective tumor clearance by *Qunatum pBac*[™] (*qPB*)-generated CAR-T cells**
347 **in Raji-bearing immunodeficient mice**

348 Next, we tested the anti-tumor potency of donor 1 and donor 2 CAR-T cells
349 in Raji-bearing immunodeficient mice (Figure 7A). Similar to the *in vitro* cytotoxicity
350 results, Raji-bearing mice injected with low, medium and high doses of donor 1
351 CAR-T cells for five days killed Raji tumor cells in a dose-dependent fashion, where

352 Raji tumors were completely eradicated by Day 5 and Day 9 in mice injected with
353 high and medium doses of donor 1 CAR-T cells, respectively (Figure 7B).



354

355 **Figure 7. *In vivo* functional characterization of CAR-T cells produced using the *Qnatum***
356 ***pBac*[™] (*qPB*) system in Raji-bearing immunodeficient mice**

357 (A) A schematic depiction showing the design of the *in vivo* functional characterization experiment.

358 (B) Bioluminescent imaging (IVIS) results showing the extent of tumor cell persistence one day

359 prior to, and five and nine days following CAR-T or Pan-T cells injection. N = 3 or 4 mice/group.

360

361 Consistent with this finding, Raji-bearing mice injected with medium dose of
362 donor 2 CAR-T cells also eradicated Raji tumor cells. Moreover, in agreement with
363 the greater *in vitro* cytotoxicity observed in donor 2 CAR-T cells (Figure 6), the Raji

364 tumor killing also appeared to have occurred at an earlier time point (at Day 5
365 following CAR-T cell injection) compared with that of donor 1 CAR-T cells (at Day
366 9 following CAR-T cell injection).

367

368 **Discussion**

369 *Sleeping Beauty* (SB) and *piggyBac* (PB) are two DNA transposons that
370 have been clinically explored recently for gene and cell therapy^{15,30}. In addition to
371 the multiple advantages over viral vectors mentioned earlier, the PB transposon
372 system has the added benefits of (1) a large cargo capacity (> 100 kb)³¹, (2) low
373 frequency of footprint-induced mutations caused by integrant remobilization³²⁻³⁴,
374 (3) being perhaps the most active transposon system in human cells³⁵, and (4)
375 being the most flexible transposon system amenable for a molecularly engineered
376 transposase to retain activity, which greatly facilitate the potential site-specific
377 genomic integration. These unique features also make *piggyBac* a superior gene
378 therapy vector over *Sleeping Beauty*. Nevertheless, *Sleeping Beauty* has been
379 considered to have less genotoxicity than *piggyBac* due to the following two
380 concerns associated with *piggyBac*. First, *piggyBac*-like terminal repeat elements
381 are prevalent in the human genome³⁶. Second, unlike a far more random genome
382 integration profile of *Sleeping Beauty*, the genome integration profile of *piggyBac* is
383 associated with euchromatin but excluded from heterochromatin^{37,38}. This
384 integration profile raises safety concerns since insertional mutagenesis of retroviral
385 vector, which was found to be due to activation of the proto-oncogene LMO2 by

386 the enhancer element of the retroviral integrant, was evident in three patients
387 enrolled in the initial SCID-X1 clinical trial.

388 The abovementioned first safety concern of *piggyBac* system was
389 thoroughly evaluated³⁹. The study demonstrated that expression of the
390 transposase alone revealed no mobilization of endogenous *piggyBac*-like
391 sequences in human genome and no increase in DNA double-strand breaks. Also,
392 no selective growth advantage of *piggyBac*-harboring cells was found in long-term
393 culture of primary human cells modified with eGFP-transposons³⁹. To address the
394 abovementioned second concern related to potential tumorigenicity induced by
395 enhancer activity of nearby integrants, we evaluated the enhancer activity of both
396 mini- and micro-*piggyBac* and identified a significantly higher level of enhancer
397 activity in the IDS region of 3' TRD in mini-*piggyBac*. Thus, by removing the IDS,
398 our micro-*piggyBac* is expected to possess significantly lower enhancer activity,
399 which in turn increases the safety profile of the donor vector. However, it has been
400 well documented that both TIRs and other sequences contained in the TRDs are
401 crucial for efficient integration of *piggyBac* transposon into the host genome.
402 Several attempts to decrease the potential genotoxicity by reducing the size of the
403 required TRDs to approximately 100 base pairs of TIRs resulted in significant
404 losses in transposition efficiency⁴⁰⁻⁴³. In contrast to these findings, our previous
405 study demonstrated that by deleting IDS from both ends and leaving only TIRs
406 (107 bp total in size), the transposition efficiency of *piggyBac* was increased by
407 2.6-fold in HEK293 when co-transfected with pPRIG-*piggyBac* which is a helper
408 plasmid expressing a CMV promoter driving bi-cistronic transcript with myc-tagged

409 wildtype *piggyBac* transposase (*PBase*) and GFP linked by IRES²⁶. However, in
410 this study, we observed that the same truncated TRDs resulted in a 2-fold
411 reduction in transposition efficiency in HEK293, Jurkat, and human primary T cells
412 when co-transfected with a different helper plasmid, a pcDNA 3.1 (control) vector
413 with a CMV promoter that drives *PBase* expression (Figure 2). These observations
414 suggest that the lowered transposition efficiency may be due to a suboptimal molar
415 ratio of donor vector and the transposases that are being co-transfected.
416 Interestingly, a marked increase in transposition efficiency can be observed in all
417 cases when the cells were co-transfected with a helper plasmid expressing
418 *qPBase v2*. This suggests that *qPBase v2* is the most robust and cell type-
419 independent *piggyBac* transposase that can achieve the highest transposition
420 activity irrespective of the type and configuration of the *piggyBac* donor vector.
421 Furthermore, the genome-wide analysis of integration sites in HEK293 cells as
422 shown in our previous study indicated that *qPBase v2* displayed a much more
423 random integration profile with no detectable hot spots, and lower preference for
424 CpG islands and cancer related genes as compared to that of *qPBase v1* and
425 wildtype *piggyBac* transposase²⁷. Collectively, these observations suggest that
426 micro-*piggyBac* in conjunction with *qPBase v2* should make a potentially safer
427 *piggyBac* system.

428 In addition to the *cis* transposon sequences (TIRs) and *trans*-elements
429 (transposase), the configuration of these *cis* and *trans* components can also highly
430 impact the transposition efficiency, safety profile, and transgene stability. For
431 example, to ensure the co-existence of the delivery cassette and transposase, a

432 single plasmid transposon system was created which places TRDs within the
433 delivery cassette, and the transposase gene in the helper part of the same
434 plasmid⁴¹. However, such an arrangement has the following disadvantages: (1)
435 reduced rate of gene delivery due to an increase in size of DNA, a phenomenon
436 particularly seen in electroporation-based gene delivery, (2) high degree of plasmid
437 backbone DNA integration when using transposon plasmids⁴¹, and (3) high rate of
438 transposase integration⁴⁴. Given these disadvantages, the *trans*-configuration
439 with two-plasmid system provides a safer and more effective transposon system.

440 However, the donor vector in a plasmid form has several undesirable qualities
441 for clinical translation, including the presence of bacterial genetic elements and
442 antibiotic-resistance genes. These undesirable risks exist because plasmid
443 backbone integration from the transposon plasmid remains a possibility.
444 Unmethylated CpG motifs highly enriched in the bacterial backbone of delivered
445 plasmids have been shown to trigger strong inflammatory responses through toll-
446 like receptor-9. These sequences will also induce transgene silencing, presumably,
447 as a result of cellular immune response⁴⁵ and/or the induction of interferon⁴⁶. To
448 reduce the chance of these events from occurring, a new *piggyBac* system was
449 established by incorporating *piggyBac* transposon into a doggyboneTM DNA
450 (dbDNA) vector, which is a linear, covalently closed, minimal DNA vector produced
451 enzymatically *in vitro*⁴⁷. A recent report has demonstrated that dbDNA, which
452 incorporates the *piggyBac* transposon system, can be used to generate stable
453 CD19-targeting CAR-T cells at a similar efficiency level compared to its plasmid
454 counterpart when a minimum of approximately 470 bp of additional randomly-

455 selected DNA flanking the transposon is included. However, due to its linear
456 configuration, dbDNA should be less efficient for electroporation-based gene
457 delivery as compared with its circular counterpart in supercoiled form. In this study,
458 we adopted the Mark Kay minicircle technology to generate the smallest *piggyBac*
459 transposon vector with TIRs (107 bp) and only 88 bp of the backbone sequence
460 flanking the TIRs. This transposon donor vector in conjunction with *qPBase v2*,
461 designated as Qunatum pBac™ (*qPB*), make the most superior *piggyBac* system
462 that is minimalistic, highly efficient, and potentially safer (Figure 3).

463 We further demonstrated that the *qPB* system can be utilized to effectively
464 generate CD19/CD20 dual-targeting CAR-T cells with 2-fold and 1.5-fold increases
465 in the percentage of CAR⁺ cells and expansion capacity, respectively, as
466 compared to those utilizing *hyPBase* (Figure 4). Additionally, the CAR-T cell
467 expansion and persistence emerged as key efficacy determinants in cancer
468 patients and both are positively correlated with the proportion of T_{SCM} in the final
469 CAR-T cell product^{48,49}. We demonstrated potent *in vitro* and *in vivo* anti-tumor
470 efficacies in *qPB*-derived CAR-T cells, which are dominated by the T_{SCM} population,
471 especially in the CD8⁺ CAR⁺ T cells. Additionally, to minimize genotoxicity caused
472 by transposase-induced integrant remobilization, transposase in a mRNA
473 configuration has been adopted in transposon-based CAR-T clinical trials⁵⁰.
474 However, as compared to transposase in DNA form, its mRNA counterpart is
475 generally less efficient, more costly for GMP production, and less stable for storage.
476 Given the low frequency of footprint-induced mutation by *piggyBac* (< 5 %) and the
477 fact that only a minimal portion (< 0.4 %) of CAR⁺ T cells expressed detectable

478 level of *qPB*ase in CAR-T cells (Figure 5B), transposase in a plasmid form should
479 be sufficiently safe when applied to highly proliferative *ex vivo*-engineered cells.
480 Additionally, our recent genome-wide integration profiling of *qPB* in CAR-T
481 products derived from two distinct donors further support its safe use in T cell
482 engineering⁵¹.

483 In summary, given its large payload capacity, high level of efficiency, and
484 outstanding safety profile, *qPB* is likely the most superior system suitable for the
485 development of next generation virus-free gene and cell therapy, especially for
486 development of multiplex CAR-T therapy.

487

488 **Materials and Methods**

489 **Human T cell samples from healthy donors**

490 Blood samples from adult healthy donors were obtained from Chang Gung
491 Memorial Hospital (Linkou, Taiwan), the acquisition of these samples was
492 approved by the Institution Review Board (IRB No. 201900578A3) at Chang Gung
493 Medical Foundation.

494 **Vector constructs**

495 Plasmids were constructed following the protocols described previously⁵²
496 and are described briefly below. Minicircle DNA were purchased from Aldevron
497 (Fargo, ND). All of the PCR products or junctions of constructs (wherever
498 sequences are ligated) were confirmed by sequencing.

499 *Vector construction*

500 **pGL3-miniP (Construct a; Figure 1A)**

501 pGL3-basic is digested with SacI and HindIII. The CMV mini-promoter with
502 SacI and HindIII sequences on its 5' and 3' ends, respectively was synthesized,
503 double-digested with SacI and HindIII, and ligated to the SacI-HindIII vector
504 fragment of pGL3-basic to make construct **a** as shown in Figure 1A.

505 **Constructs b-e (Figure 1A)**

506 pGL3-miniP was digested with KpnI and XhoI. The 5'TIR or 3'TIR of micro-
507 *piggyBac* or 5'TRD or 3'TRD of mini-*piggyBac* with kpnI and XhoI sequences
508 added on either end was synthesized, double-digested with KpnI and XhoI, and
509 ligated to the KpnI-XhoI vector fragment of pGL3-miniP, respectively, to make the
510 set of constructs (**b-e**) for evaluation of enhancer activity of mini-*piggyBac*'s and
511 micro-*piggyBac*'s TRDs and TIRs, respectively.

512 **Donor vectors (Figure 2A)**

513 "Mini-*piggyBac*-Long" is the same construct as the donor of *piggyBac*
514 system published previously²⁰

515 "Micro-*piggyBac*-Short" is the plasmid named "*pPB*-cassette short" as published
516 previously²⁶

517 "Micro-*piggyBac*-Long" is constructed by replacing the backbone of "micro-
518 *piggyBac*-Short" with that of "mini-*piggyBac*-Long" via PCR-based cloning.

519 **Helper plasmid (Figure 2A)**

520 The construction of helper plasmid was described previously²⁷.

521 **Parental *qPB* donor vector (Figure 3A)**

522 The parental plasmid contains the sequences of the following components
523 (obtained by DNA synthesis) arranged in a 5' to 3' order: Kanamycin resistance

524 gene, origin of replication (pMB1), 32 I-SceI sites, attB site (PhiC31), 5'TIR of
525 micro-*piggyBac*, multiple cloning site (MSC), 3'TIR of micro-*piggyBac*, and attP
526 site (PhiC31).

527 **pQ-tdTomato-IRES-hygro (Figure 3A)**

528 The DNA for a cassette with the CAG promoter driving a bi-cistronic
529 transcript containing tdTomato gene, internal ribosome entry site (IRES) of Foot-
530 and-mouth disease virus (FMDV), and hygromycin resistance gene was
531 synthesized and cloned into the AseI and EcoRV site of the parental *qPB* vector
532 to make pQ-tdTomato-IRES-hygro.

533 **pQ-CD20CD19CAR (Figure 4A)**

534 The dual-targeting tandem CD20/CD19 CAR-containing pQ-
535 CD20CD19CAR vector encodes a second-generation CAR composed by an
536 elongation factor 1-alpha ($EF1\alpha$) promoter which drives an extracellular domain
537 derived from the single chain variable fragments (scFv) of monoclonal antibodies
538 directed against the CD19 and CD20 antigens, respectively, and further linked to
539 the CD3z chain of the TCR complex by means of a CD8 hinge and transmembrane
540 domains, together with the 4-1BB co-stimulatory domain. Following synthesis, the
541 expression cassette is cloned into the MCS of parental *qPB* vector to make pQ-
542 CD20CD19CAR.

543 **Minicircle DNA**

544 The minicircle DNAs, Q-tdTomato-IRES-hygro (Figure 3A) and Q-
545 CD20CD19CAR (Figure 4A), are manufactured by Aldevron from their parental
546 plasmid, pQ-tdTomato-IRES-hygro and pQ-CD2019CAR, respectively.

547 ***qPB*Base**

548 To comply with the FDA regulations, the ampicillin gene in the helper
549 plasmid expressing *qPB*Base v2 was replaced by a kanamycin resistance gene
550 sequence to make *qPB*Base. *qPB*Base combines with *qPB* donor vector (minicircle
551 DNA) to form the *qPB* system.

552 **Enhancer assay**

553 The control, pPL-TK (Renilla Luciferase), was co-transfected with the
554 specified firefly luciferase constructs (i.e., pGL3-miniP, pGL3-miniP-microL, pGL3-
555 miniP-microR, pGL3-miniP-miniR, pGL3-miniP-miniL, mini-*piggyBac* Long, micro-
556 *piggyBac* Short, or micro-*piggyBac* Long) by either FuGENE (HEK293) or
557 nucleofection (Sf9 cells, and Jurkat T cells). In some experiments, constructs were
558 first linearized utilizing a XmnI or Bgl I restriction enzyme. Forty-eight hours after
559 transfection, cells were harvested and subjected to Dual-Luciferase assay
560 (Promega) by following the manufacturing instructions.

561 **Transposition assay**

562 HEK293 cells (1×10^5) were transfected with 200-334 ng of donor vector
563 carrying a hygromycin resistance gene and 200-282 ng of helper plasmid in MEM
564 medium (GeneDireX), 10% FBS (Corning) utilizing the X-tremeGENE™ HP DNA
565 transfection reagent (Merck). Transfected cells were transferred to 100-mm plates
566 and cultured under hygromycin (100 μ g/ml) selection pressure for 14 days. Cells
567 were then harvested and fixed with 4% paraformaldehyde. Fixed cells were stained
568 with 0.2% methylene blue and cell colonies were enumerated.

569 Jurkat or primary T cells (2×10^5) were electroporated with 400-668 ng of donor
570 vector carrying a hygromycin resistance gene which in some experiments was also
571 linked to a tdTomato gene, and 400-517 ng of helper plasmid in OpTmizer medium
572 supplemented with *Quantum Booster*[™] (GenomeFrontier). Electroporation was
573 carried out using a 4D-Nucleofector[™] (Lonza) in combination with the *Quantum*
574 *Nufect*[™] Kit (GenomeFrontier) according to the manufacturer's instructions.
575 Electroporated cells were transferred to 96-well plates and cultured under
576 hygromycin (1 mg/ml) selection pressure for 14 days. Cells were then harvested
577 and stained with AO/PI. Live cell numbers were determined using Celigo image
578 cytometry (Nexcelom). Transposition efficiency was expressed as number of
579 hygromycin-resistant colonies or live cells.

580 **Generation and expansion of CAR-T cells**

581 Peripheral blood mononuclear cells (PBMCs) were isolated from blood
582 samples of healthy donors by utilizing Ficoll-Hypaque gradient separation. CD3⁺ T
583 cells were isolated from PBMCs using EasySep[™] Human T Cell Isolation Kit
584 (StemCell Technologies) according to the manufacturer's instructions. T cells were
585 activated by co-incubation with Dynabeads[™] (Invitrogen) in X-VIVO 15 medium
586 (Lonza) for two days at a beads to cells ratio of 3:1. Following the removal of
587 Dynabeads[™], activated T cells were harvested and frozen down or utilized in
588 experiments. Electroporation of activated T cells was carried out using a
589 Nucleofector[™] 2b Device (Lonza) in combination with the *Quantum Nufect*[™] Kit
590 (GenomeFrontier) according to the manufacturer's instructions. Cells were
591 electroporated with the combination of CD20/CD19 CAR donor vector, and pCMV-

592 *hyPBase* or pCMV-*qPBase v2* helper vector. Cells were cultured and expanded
593 for 10 or 14 days in OpTmizer medium (Thermo Fisher Scientific) supplemented
594 with 50 IU of IL-2 (PeproTech) and 10% FBS, and thereafter harvested for
595 experiment. γ -irradiated aAPC were added on Day 3 to the T cell expansion
596 cultures at a aAPC:T cell ratio of 1:1.

597 **Evaluation of CAR-T cells performance**

598 CAR expression on T cells was determined by flow cytometry analysis
599 following staining of cells at 4°C for 30 minutes with F(ab')₂ fragment specific,
600 biotin-conjugated goat anti-mouse antibodies (Jackson ImmunoResearch
601 Laboratories) and R-phycoerythrin (PE)-conjugated streptavidin (Jackson
602 ImmunoResearch Laboratories). Similarly, cells were also stained with the
603 following antigen-specific antibodies: CD3-Pacific Blue, CD4-Alexa Flour 532
604 (Thermo Fisher Scientific), CD8-PE-Cy7, CD45RA-BV421, CD62L-PE-Cy5, or
605 CD95-BV711 (Biolegend). Cells may also be incubated with propidium iodide (PI,
606 Thermo Fisher Scientific) and/or Acridine orange (AO, Nexcelom). PI⁻ cells and T
607 cell differentiation subsets were determined by flow cytometry based on CD45RA,
608 CD62L and CD95 expression: T_N (CD45RA⁺CD62L⁺CD95⁻), T_{SCM}
609 (CD45RA⁺CD62L⁺CD95⁺), T_{CM} (CD45RA⁻CD62L⁺), T_{EM} (CD45RA⁻CD62L⁻), and
610 T_{EFF} (CD45RA⁺CD62L⁻). *qPBase* is expressed as a fusion protein of GFP and
611 transposase. Its expression was determined by flow cytometry analysis of GFP⁺
612 cells. In some experiments a hygromycin resistant gene was expressed with a
613 tdTomato gene and hygromycin resistant cells was determined by flow cytometry
614 analysis of tdTomato⁺ cells. Flow cytometric measurements and analyses were

615 performed on a SA3800 Spectral Analyzer (Sony). Histograms and dot-plots were
616 generated using GraphPad Prism software (GraphPad). Live cells were
617 determined using Celigo image cytometry (Nexcelom) and represent the number
618 of AO⁺, PI⁻ cells.

619 ***In vitro* cytotoxicity assay**

620 Target antigen-expressing cells were engineered as according to the
621 method described elsewhere⁵¹. 5 x 10³ cells per well of CD19⁺ (K562 CD19-
622 tdTomato), CD20⁺ (K562 CD20-GFP), CD19⁺CD20⁺ (Raji-GFP) or non-relevant
623 K562 BCMA-GFP target cells were seeded in 96-well culture plates (Corning) and
624 control Pan-T or CAR-T cells were added at an E:T ratio of 5:1, 1:1, 1:3 or 1:10.
625 CAR-T cells mediated cytotoxicity on target cells was then assessed by using
626 Celigo image cytometry (Nexcelom) to determine the number of live target cells at
627 0, 24, 48, 72 and 96 hours after co-culturing. Cell aggregates were separated by
628 pipetting before Celigo imaging. The percent of specific lysis for each sample was
629 calculated using the formula: [1-(live fluorescent cell count in the presence of target
630 cells and CAR-T cells / live fluorescent cell count in the presence of target cells
631 only)] x 100.

632 ***In vitro* cytokine release assay**

633 Pan-T control cells or CAR-T cells produced from two healthy donors were
634 thawed and added to cultures containing CD19⁺ (K562 CD19-tdTomato), CD20⁺
635 (K562 CD20-GFP), CD19⁺CD20⁺ (Raji-GFP) or non-relevant K562 BCMA-GFP
636 tumor target cells. The cells were added at an effector:target (E:T) ratio of 10:1 in
637 OpTmizer medium supplemented with 50 IU of IL-2 and 10% FBS. Following 48 h

638 of co-culture, supernatant was collected and IFN- γ levels in the culture supernatant
639 was measured by performing enzyme-linked immunosorbent assay (Thermo
640 Fisher) according to the manufacturer's instructions.

641 **Mouse xenograft model**

642 *In vivo* studies using mouse xenograft model were conducted at the
643 Development Center for Biotechnology, Taiwan, using animal protocols approved
644 by the Taiwan Mouse Clinic IACUC (2020-R501-035). Briefly, eight-week-old
645 female ASID (NOD.Cg-Prkdc^{scid}Il2rg^{tm1Wjl}/YckNarl) mice (National Laboratory
646 Animal Center, Taiwan) were intravenously (i.v.) injected with 1.5×10^5 Raji-
647 Luc/GFP tumor cells. One week after Raji-Luc/GFP tumor cell injection, mice were
648 injected with 3×10^6 CAR-T cells or control Pan-T cells. Luminescence signals
649 from Raji-Luc/GFP tumor cells was monitored using the Xenogen-IVIS Imaging
650 System (Caliper Life Sciences).

651 **Statistical analysis**

652 Statistical analyses of differences between two groups and among three or
653 more groups were carried out using the Student's t-test (two-tailed) and the one-
654 way ANOVA with Tukey's multiple comparison test, respectively. The analyses
655 were performed using GraphPad Prism software (GraphPad Software), and
656 statistical significance was reported as * $p < 0.05$, ** $p < 0.01$, and *** $p < 0.001$.
657 Differences are considered to be statistically significant when $p < 0.05$.

658

659 **Acknowledgments, funding source and materials sharing**

660 The authors thank Ms. Lu-Chun Chen for her assistance throughout the IRB
661 preparation and approval process. The authors also thank Dr. Pei-Yi Tsai for
662 assistance with the animal experiments. This study is funded by GenomeFrontier
663 Therapeutics, Inc. Due to company policy, proprietary materials cannot be widely
664 distributed to the public. GenomeFrontier welcomes inquiries to request samples
665 for testing.

666

667 **Author Contributions:**

668 S.C.-Y.W. designed research. Y.-C.C.(Yi-Chun Chen), P.-N.W., Y.-S.Y., Y.-
669 C.C.(Ying-Chun Chen), I.-C.C. performed research. W.-K.H., Y.-C.C.(Yi-Chun
670 Chen), J.C.H., K.-L.K.W., and S.C.-Y.W. analyzed data. J.C.H., P.S.C. and S.C.-
671 Y.W. wrote the paper.

672

673 **Declaration of Interests Statement:**

674 S.C.-Y.W. is the founder of GenomeFrontier Therapeutics, Inc., W.-K.H.,
675 Y.-C.C.(Yi-Chun Chen), K.-L.K.W., Y.-S.Y., Y.-C.C.(Ying-Chun Chen), I.-C.C., and
676 J.C.H. are affiliated with GenomeFrontier Therapeutics, Inc.

677

678 **References**

679

- 680 1. Strachan, T., and Read, A. (2020). Mapping Genes Conferring Susceptibility to Complex
681 Diseases. In *Human Molecular Genetics*, pp. 467–496.
- 682 2. Ghosh, S., Brown, A.M., Jenkins, C., and Campbell, K. (2020). Viral Vector Systems for
683 Gene Therapy: A Comprehensive Literature Review of Progress and Biosafety Challenges.
684 *Applied Biosafety* 25, 7–18.
- 685 3. Nowrouzi, A., Glimm, H., von Kalle, C., and Schmidt, M. (2011). Retroviral vectors: Post
686 entry events and genomic alterations. *Viruses* 3, 429–455.
- 687 4. Schröder, A.R.W., Shinn, P., Chen, H., Berry, C., Ecker, J.R., and Bushman, F. (2002). HIV-1
688 integration in the human genome favors active genes and local hotspots. *Cell* 110, 521–
689 529.
- 690 5. Cesana, D., Sgualdino, J., Rudilosso, L., Merella, S., Naldini, L., and Montini, E. (2012).
691 Whole transcriptome characterization of aberrant splicing events induced by lentiviral
692 vector integrations. *Journal of Clinical Investigation* 122, 1667–1676.
- 693 6. Modlich, U., Navarro, S., Zychlinski, D., Maetzig, T., Knoess, S., Brugman, M.H.,
694 Schambach, A., Charrier, S., Galy, A., Thrasher, A.J., et al. (2009). Insertional
695 transformation of hematopoietic cells by self-inactivating lentiviral and gammaretroviral
696 vectors. *Molecular Therapy* 17, 1919–1928.
- 697 7. Hacein-Bey-Abina, S., Garrigue, A., Wang, G.P., Soulier, J., Lim, A., Morillon, E., Clappier,
698 E., Caccavelli, L., Delabesse, E., Beldjord, K., et al. (2008). Insertional oncogenesis in 4
699 patients after retrovirus-mediated gene therapy of SCID-X1. *Journal of Clinical*
700 *Investigation* 118, 3132–3142.
- 701 8. Cesana, D., Ranzani, M., Volpin, M., Bartholomae, C., Duros, C., Artus, A., Merella, S.,
702 Benedicenti, F., Sergi Sergi, L., Sanvito, F., et al. (2014). Uncovering and dissecting the
703 genotoxicity of self-inactivating lentiviral vectors in vivo. *Molecular Therapy* 22, 774–785.
- 704 9. Jähner, D., and Jaenisch, R. (1985). Retrovirus-induced de novo methylation of flanking
705 host sequences correlates with gene inactivity. *Nature* 315, 594–597.
- 706 10. Jähner, D., Stuhlmann, H., Stewart, C.L., Harbers, K., Löhler, J., Simon, I., and Jaenisch, R.
707 (1982). De novo methylation and expression of retroviral genomes during mouse
708 embryogenesis. *Nature* 298, 623–628.
- 709 11. Raper, S.E., Chirmule, N., Lee, F.S., Wivel, N.A., Bagg, A., Gao, G.P., Wilson, J.M., and
710 Batshaw, M.L. (2003). Fatal systemic inflammatory response syndrome in a ornithine
711 transcarbamylase deficient patient following adenoviral gene transfer. *Molecular*
712 *Genetics and Metabolism* 80, 148–158.
- 713 12. van der Loo, J.C.M., and Wright, J.F. (2016). Progress and challenges in viral vector
714 manufacturing. *Hum Mol Genet* 25, R42–R52.

- 715 13. Ramamoorth, M., and Narvekar, A. (2015). Non viral vectors in gene therapy - An
716 overview. *Journal of Clinical and Diagnostic Research* 9, GE01–GE06.
- 717 14. Meir, Y.J.J., and Wu, S.C.Y. (2011). Transposon-based vector systems for gene therapy
718 clinical Trials: Challenges and considerations. *Chang Gung Medical Journal* 34, 565–579.
- 719 15. Tipanee, J., Chai, Y.C., Driessche, T. vanden, and Chuah, M.K. (2017). Preclinical and
720 clinical advances in transposon-based gene therapy. *Bioscience Reports* 37,
721 BSR20160614.
- 722 16. Ivics, Z., Hackett, P.B., Plasterk, R.H., and Izsvák, Z. (1997). Molecular reconstruction of
723 sleeping beauty, a Tc1-like transposon from fish, and its transposition in human cells. *Cell*
724 91, 501–510.
- 725 17. Ivics, Z., and Izsvák, Z. (2005). A whole lotta jumpin’ goin’ on: New transposon tools for
726 vertebrate functional genomics. *Trends in Genetics* 21, 8–11.
- 727 18. Fraser, M.J., Smith, G.E., and Summers, M.D. (1983). Acquisition of Host Cell DNA
728 Sequences by Baculoviruses: Relationship Between Host DNA Insertions and FP Mutants
729 of *Autographa californica* and *Galleria mellonella* Nuclear Polyhedrosis Viruses. *Journal of*
730 *Virology* 47, 287–300.
- 731 19. Ding, S., Wu, X., Li, G., Han, M., Zhuang, Y., and Xu, T. (2005). Efficient transposition of
732 the piggyBac (PB) transposon in mammalian cells and mice. *Cell* 122, 473–483.
- 733 20. Wu, S.C.Y., Meir, Y.J.J., Coates, C.J., Handler, A.M., Pelczar, P., Moisyadi, S., and Kaminski,
734 J.M. (2006). piggyBac is a flexible and highly active transposon as compared to Sleeping
735 Beauty, Tol2, and Mos1 in mammalian cells. *Proc Natl Acad Sci U S A* 103, 15008–15013.
- 736 21. Mátés, L., Chuah, M.K.L., Belay, E., Jerchow, B., Manoj, N., Acosta-Sanchez, A., Grzela,
737 D.P., Schmitt, A., Becker, K., Matrai, J., et al. (2009). Molecular evolution of a novel
738 hyperactive Sleeping Beauty transposase enables robust stable gene transfer in
739 vertebrates. *Nature Genetics* 41, 753–761.
- 740 22. Voigt, F., Wiedemann, L., Zuliani, C., Querques, I., Sebe, A., Mátés, L., Izsvák, Z., Ivics, Z.,
741 and Barabas, O. (2016). Sleeping Beauty transposase structure allows rational design of
742 hyperactive variants for genetic engineering. *Nature Communications* 7, 11126.
- 743 23. Cadiñanos, J., and Bradley, A. (2007). Generation of an inducible and optimized piggyBac
744 transposon system. *Nucleic Acids Research* 35, e87.
- 745 24. Yusa, K., Zhou, L., Li, M.A., Bradley, A., and Craig, N.L. (2011). A hyperactive piggyBac
746 transposase for mammalian applications. *Proc Natl Acad Sci U S A* 108, 1531–1536.
- 747 25. Yusa, K. (2015). piggyBac transposon. In *Mobile DNA III* (ASM Press), pp. 873–890.
- 748 26. Meir, Y.J.J., Weirauch, M.T., Yang, H.S., Chung, P.C., Yu, R.K., and Wu, S.C.Y. (2011).
749 Genome-wide target profiling of piggyBac and Tol2 in HEK 293: Pros and cons for gene
750 discovery and gene therapy. *BMC Biotechnology* 11, 28.

- 751 27. Meir, Y.J.J., Lin, A., Huang, M.F., Lin, J.R., Weirauch, M.T., Chou, H.C., Lin, S.J.A., and Wu,
752 S.C.Y. (2013). A versatile, highly efficient, and potentially safer piggyBac transposon
753 system for mammalian genome manipulations. *FASEB Journal* 27, 4429–4443.
- 754 28. Cooney, A.L., Singh, B.K., and Sinn, P.L. (2015). Hybrid nonviral/viral vector systems for
755 improved piggyBac DNA transposon in vivo delivery. *Molecular Therapy* 23, 667–674.
- 756 29. Kay, M.A., He, C.Y., and Chen, Z.Y. (2010). A robust system for production of minicircle
757 DNA vectors. *Nature Biotechnology* 28, 1287–1289.
- 758 30. Magnani, C.F., Tettamanti, S., Alberti, G., Pisani, I., Biondi, A., Serafini, M., and Gaipa, G.
759 (2020). Transposon-Based CAR T Cells in Acute Leukemias: Where are We Going? *Cells* 9,
760 1337.
- 761 31. Li, R., Zhuang, Y., Han, M., Xu, T., and Wu, X. (2013). PiggyBac as a high-capacity
762 transgenesis and gene-therapy vector in human cells and mice. *DMM Disease Models*
763 and Mechanisms 6, 828–833.
- 764 32. Elick, T.A. (1996). Excision of the piggy Bac transposable element in vitro is a precise
765 event that is enhanced by the expression of its encoded transposase. *Genetica* 98, 33–41.
- 766 33. Li, M.A., Pettitt, S.J., Eckert, S., Ning, Z., Rice, S., Cadiñanos, J., Yusa, K., Conte, N., and
767 Bradley, A. (2013). The piggyBac Transposon Displays Local and Distant Reintegration
768 Preferences and Can Cause Mutations at Noncanonical Integration Sites. *Molecular and*
769 *Cellular Biology* 33, 1317–1330.
- 770 34. Chen, Q., Luo, W., Veach, R.A., Hickman, A.B., Wilson, M.H., and Dyda, F. (2020).
771 Structural basis of seamless excision and specific targeting by piggyBac transposase.
772 *Nature Communications* 11, 3446.
- 773 35. Doherty, J.E., Huye, L.E., Yusa, K., Zhou, L., Craig, N.L., and Wilson, M.H. (2012).
774 Hyperactive piggybac gene transfer in human cells and in vivo. *Human Gene Therapy* 23,
775 311–320.
- 776 36. Feschotte, C. (2006). The piggyBac transposon holds promise for human gene therapy.
777 *Proc Natl Acad Sci U S A* 103, 14981–14982.
- 778 37. Galvan, D.L., Nakazawa, Y., Kaja, A., Kettlun, C., Cooper, L.J.N., Rooney, C.M., and Wilson,
779 M.H. (2009). Genome-wide mapping of piggybac transposon integrations in primary
780 human T cells. *Journal of Immunotherapy* 32, 837–844.
- 781 38. Hamada, M., Nishio, N., Okuno, Y., Suzuki, S., Kawashima, N., Muramatsu, H., Tsubota, S.,
782 Wilson, M.H., Morita, D., Kataoka, S., et al. (2018). Integration Mapping of piggyBac-
783 Mediated CD19 Chimeric Antigen Receptor T Cells Analyzed by Novel Tagmentation-
784 Assisted PCR. *EBioMedicine* 34, 18–26.
- 785 39. Saha, S., Woodard, L.E., Charron, E.M., Welch, R.C., Rooney, C.M., and Wilson, M.H.
786 (2015). Evaluating the potential for undesired genomic effects of the piggyBac
787 transposon system in human cells. *Nucleic Acids Research* 43, 1770–1782.

- 788 40. Li, X., Harrell, R.A., Handler, A.M., Beam, T., Hennessy, K., and Fraser, M.J. (2005).
789 piggyBac internal sequences are necessary for efficient transformation of target
790 genomes. *Insect Molecular Biology* 14, 17–30.
- 791 41. Solodushko, V., Bitko, V., and Fouty, B. (2014). Minimal piggyBac vectors for chromatin
792 integration. *Gene Therapy* 21, 1–9.
- 793 42. Elick, T.A., Lobo, N., and Fraser, M.J. (1997). Analysis of the cis-acting DNA elements
794 required for piggyBac transposable element excision. *Molecular and General Genetics*
795 255, 605–610.
- 796 43. Li, X., Lobo, N., Bauser, C.A., and Fraser, M.J. (2001). The minimum internal and external
797 sequence requirements for transposition of the eukaryotic transformation vector
798 piggyBac. *Molecular Genetics and Genomics* 266, 190–198.
- 799 44. Urschitz, J., Kawasumi, M., Owens, J., Morozumi, K., Yamashiro, H., Stoytchev, I., Marh, J.,
800 Dee, J.A., Kawamoto, K., Coates, C.J., et al. (2010). Helper-independent piggyBac plasmids
801 for gene delivery approaches: Strategies for avoiding potential genotoxic effects. *Proc*
802 *Natl Acad Sci U S A* 107, 8117–8122.
- 803 45. Chen, Z.Y., Yant, S.R., He, C.Y., Meuse, L., Shen, S., and Kay, M.A. (2001). Linear DNAs
804 concatemerize in vivo and result in sustained transgene expression in mouse liver.
805 *Molecular Therapy* 3, 403–410.
- 806 46. Huerfano, S., Ryabchenko, B., and Forstová, J. (2013). Nucleofection of expression
807 vectors induces a robust interferon response and inhibition of cell proliferation. *DNA and*
808 *Cell Biology* 32, 467–479.
- 809 47. Bishop, D.C., Caproni, L., Gowrishankar, K., Legiewicz, M., Karbowiczek, K., Tite, J.,
810 Gottlieb, D.J., and Micklethwaite, K.P. (2020). CAR T Cell Generation by piggyBac
811 Transposition from Linear Doggybone DNA Vectors Requires Transposon DNA-Flanking
812 Regions. *Molecular Therapy - Methods and Clinical Development* 17, 359–368.
- 813 48. Gattinoni, L., Speiser, D.E., Lichterfeld, M., and Bonini, C. (2017). T memory stem cells in
814 health and disease. *Nature Medicine* 23, 18–27.
- 815 49. Biasco, L., Izotova, N., Rivat, C., Ghorashian, S., Richardson, R., Guvenel, A., Hough, R.,
816 Wynn, R., Popova, B., Lopes, A., et al. (2021). Clonal expansion of T memory stem cells
817 determines early anti-leukemic responses and long-term CAR T cell persistence in
818 patients. *Nature Cancer* 2, 629–642.
- 819 50. Prommersberger, S., Reiser, M., Beckmann, J., Danhof, S., Amberger, M., Quade-Lyssy, P.,
820 Einsele, H., Hudecek, M., Bonig, H., and Ivics, Z. (2021). CARAMBA: a first-in-human
821 clinical trial with SLAMF7 CAR-T cells prepared by virus-free Sleeping Beauty gene
822 transfer to treat multiple myeloma. *Gene Therapy* 28, 560–571.
- 823 51. Chen, Y.-C., Hua, W.-K., Hsu, J.C., Chang, P.S., Karen Wen, K.-L., Huang, Y.-W., Tsai, J.-C.,
824 Kao, Y.-H., Wu, P.-H., Wang, P.-N., et al. (2022). Quantum CART (qCART), a piggyBac-
825 based system for development and production of virus-free multiplex CAR-T cell therapy.

826 52. Sambrook, J., and Russell, D.W. (2001). Molecular Cloning: A Laboratory Manual, Third
827 Edition. In Molecular Cloning: a laboratory a manual, pp. 1.32-1.34.

828